THREE-DIMENSIONAL BENT-GRAVITY WAVES WITH NON-UNIFORM COMPRESSION

A. E. Bukatov, V. V. Zharkov, and D. D. Zav'yalov

UDC 532.593:539.3:624.131

The effect of nonuniform compression on three-dimensional bending oscillations for a thin elastic floating plate and wave disturbance in a layer of uniform liquid beneath it with movement of the pressure field is studied. The dependence of the hodograph of the wave vector and the structure of the phase portraits of oscillations on the displacement velocity and direction of the wave generator, and values of the longitudinal, transverse, and shear compressive forces is analyzed. Bent-gravity waves with movement of the pressure field for conditions of longitudinal and transverse compression have been studied in [1-4].

1. Let at the flow surface of a uniform ideal incompressible liquid of constant depth H float a thin elastic nonuniform compressed plate. Over the surface of the plate at angle α to the direction of flow a wave disturbance generator moves with constant velocity v

$$p = p_0 f(x_1, y) \exp(-i\sigma t), \quad x_1 = x - vt. \tag{1.1}$$

We consider the effect of compressive forces on three-dimensional steady-state bending oscillations of the plate and wave disturbance of the liquid flow. On coordinate system x_1, y, z, connected with moving pressure field (1.1) the problem of low amplitude vibrations is reduced to solving the Laplace equation

$$\Delta\varphi = 0, \quad -H < z < 0 \tag{1.2}$$

with boundary conditions

$$\begin{gathered} L\zeta + (1/g)F\varphi = p_1 f(x, y) \exp(-i\sigma t), \ z = 0; \\ F\zeta = \partial\varphi/\partial z, \ z = 0; \ \partial\varphi/\partial z = 0, \ z = -H. \end{gathered} \tag{1.3}$$

Here

$$L = D_1\nabla^4 + Q_1\frac{\partial^2}{\partial x^2} + Q_2\frac{\partial^2}{\partial y^2} + 2Q_3\frac{\partial^2}{\partial x\,\partial y} + \varkappa_1 F^2 + 1;$$

$$F = \frac{\partial}{\partial t} + (u_x + v)\frac{\partial}{\partial x} + u_y\frac{\partial}{\partial y}; \ \nabla^2 = \frac{\partial^2}{\partial x^2} + \frac{\partial^2}{\partial y^2};$$

$$\{D_1, Q_1, Q_2, Q_3, \varkappa_1, p_1\} = \frac{1}{\rho g}\{D, Q_x, Q_y, Q_{xy}, \varkappa, p_0\};$$

$$D = Eh^3[12(1-\nu^2)]^{-1}; \ \varkappa = \rho_1 h; \ u_x = u\cos\alpha; \ u_y = u\sin\alpha;$$

Q_x, Q_y, Q_{xy} are compressive forces in the corresponding directions; E, h, ν, ρ_1 are normal elasticity modulus, thickness, Poisson's ratio, and plate density; ρ is liquid density; u is flow velocity vector modulus; ζ is plate deflection. Here and subsequently the index 1 for x_1 is omitted.

By solving problem (1.1)-(1.3) by the method of Fourier integral transformation for plate deflection ζ we obtain an expression

$$\zeta = \frac{p_1}{2\pi}\int_{-\infty}^{\infty}\int \frac{\bar{f}(m, n)\,M(r)}{\tau^2 - \sigma_0^2}\exp[i(mx + ny - \sigma t)]\,dm\,dn, \tag{1.4}$$

$$\tau^2 = M(r)l(m, n), \ M(r) = (1 + \varkappa_1 rg\ \mathrm{th}\ rH)^{-1}rg\ \mathrm{th}\ rH,$$
$$l(m, n) = 1 + D_1 r^4 - Q_1 m^2 - Q_2 n^2 - 2Q_3 mn,$$
$$\sigma_0 = \sigma - (u_x + v)m - u_y n, \ r^2 = m^2 + n^2$$

($\bar{f}(m, n)$ is the Fourier transform of function $f(x, y)$).

The equation $\tau^2 - \sigma_0^2 = 0$ connecting wave number r with frequency σ, flow velocity u, and the rate of disturbance source displacement v determines the hodograph of the wave vector

Sevastopol. Translated from Prikladnaya Mekhanika i Tekhnicheskaya Fizika, No. 6, pp. 51-57, November-December, 1991. Original article submitted May 3, 1990, revision resubmitted, August 24, 1990.

0021-8944/91/3206-0867$12.50

in plane (m, n). Steady-state wave disturbances in a distant zone described by expression (1.4) are characterized [5, 6] by coordinates (m, n) of the hodograph G(m, n) = 0.

2. We consider a source of constant intensity ($\sigma = 0$) moving over the surface of the plate with absence of drift ($u = 0$). Then it is possible to reduce the equation for the hodograph to the form

$$m = \{[S_1S_2 + 2S_3[S_3r^2 \pm (S_3^2r^4 + S_1S_2r^2 - S_1^2)^{1/2}]](S_2^2 + 4S_3^2)^{-1}\}^{1/2},$$

$$n = \pm(r^2 - m^2)^{1/2} \operatorname{sign} Q_3,$$

$$S_1 = rg(1 + D_1r^4 + Q_2r^2) \operatorname{th} rH,\ S_2 = v^2(1 + \varkappa_1 rg \operatorname{th} rH) + (Q_1 - Q_2)rg \operatorname{th} rH,$$

$$S_3 = Q_3 rg \operatorname{th} rH.$$

The upper and lower signs at n and in the square brackets for the expression of m relate to arcs of the hodograph which lie respectively above and below the abscissa axis. The hodograph is determined with $v > v_0$, where

$$v_0 = \Phi(r_0),\ \Phi'(r_0) = 0,\ \Phi(r) = \frac{1}{r}\left\{M(r)\left[(1+D_1r^4-Q_1r^2) - \frac{(r^2Q_3)^2}{1+D_1r^4-Q_2r^2}\right]\right\}^{1/2}.$$

If $Q_3 = 0$, then $m = (S_1/S_2)^{1/2}$, $n = \pm (r^2 - m^2)^{1/2}$ and the hodograph is symmetrical with respect to the abscissa axis. In addition Q_2 does not affect v_0, and the dependence of this critical velocity on Q_1 is considered in [7].

3. In order to study the dependence of the hodograph and structure of wave disturbances on the magnitude of longitudinal, transverse, and shear compressive forces numerical calculations were made with different displacement velocities for the source of the disturbance for the values $E = 5 \cdot 10^9$ N/m^2, $H = 350$ m; $h = 2.5$ m, $\nu = 0.34$, $\rho_1 = 870$ kg·m^{-3}, $\rho = 1025$ kg·m^{-3}, which characterize an ice plate [8, 9].

Analysis of the results of numerical calculations showed that with $Q_3 \neq 0$ the distribution of v_0 with respect to Q_1 is qualitatively similar to the distribution in the case of uniform compression. The quantitative dependence of v_0 on Q_1 for $Q_2 = 0$, $Q_3 \geq 0$ is given in Table 1, where $Q_0 = \sqrt{D_1}$. The role of Q_3 indepedent of its sign appears in a reduction in v_0. Transverse compression (tension) with consideration of shear forces ($Q_3 \neq 0$) reduces (increases) v_0, and the effect of Q_2 is reinforced with an increase in Q_3. The distribution of v_0 with respect to Q_2 and Q_3 is illustrated in Fig. 1 (solid, broken, broken-dotted, and dotted lines relate to $Q_1 = Q_3 = 0$; $Q_1 = 0$, $Q_3 = 0$; $Q_1 = 0$, $Q_3 = (3/2)Q_0$; $Q_1 = Q_3 = Q_0$ (a), $Q_1 = Q_2 = 0$; $Q_1 = 0$, $Q_2 = (3/2)Q_0$; $Q_1 = (3/2)Q_0$, $Q_2 = 0$; $Q_1 = Q_2 = (3/2)Q_0$ (b)). It can be seen that in the presence of shear forces there is the possibility of conditions for generation of wave disturbances by a source moving with any non-zero velocity.

Hodographs of the wave vector without taking account of and with consideration of shear forces are presented in Figs. 2 and 3 respectively with $v = 45$ m·sec^{-1} from the range $v_0 < v < c$ ($c = \sqrt{gH}$). Lines 1-5 correspond to $Q_1 = Q_2 = 0$; $Q_1 = -Q_0$, $Q_2 = Q_0$; $Q_1 = 2Q_0$, $Q_2 = 0$; $Q_1 = 0$, $Q_2 = 1{,}9Q_0$; $Q_1 = Q_0$, $Q_2 = -Q_0$ (Fig. 2) and $Q_1 = Q_2 = Q_3 = 0$; $Q_1 = Q_2 = Q_3 = Q_0$; $Q_1 = Q_2 = 0$, $Q_3 = Q_0$; $Q_1 = Q_2 = 0$, $Q_3 = 2Q_0$; $Q_1 = 0$, $Q_2 = 1.9Q_0$, $Q_3 = 1.5Q_0$ (Fig. 3). It can be seen that for all hodographs the presence of two points of inflection is typical in both the upper and lower half planes. In hodographs where the breaks are particularly clear these points are marked by circles and triangles, and the asterisks are points of contact of a hodograph and a beam emerging from the origin. A reduction in v leads to convergence of the points of inflection on arcs of the hodograph in the upper and lower half planes. Merging of these points for $Q_3 = 0$ occurs with velocity $v = v_1$ determined from the set of equations

$$n''m' - n'm'' = 0; \quad n'''m' - n'm''' = 0 \tag{3.1}$$

TABLE 1

Q_1/Q_0	Q_3/Q_0		
	0	1	1,5
−2	29,065	28,037	26,196
−1,5	27,589	26,309	24,061
−1	25,915	24,332	21,593
−0,5	24,011	22,039	18,668
0	21,797	19,318	15,030
0,5	19,157	15,959	9.227
1	15,869	11,413	0
1,5	11,381	0	0
2	0	0	0

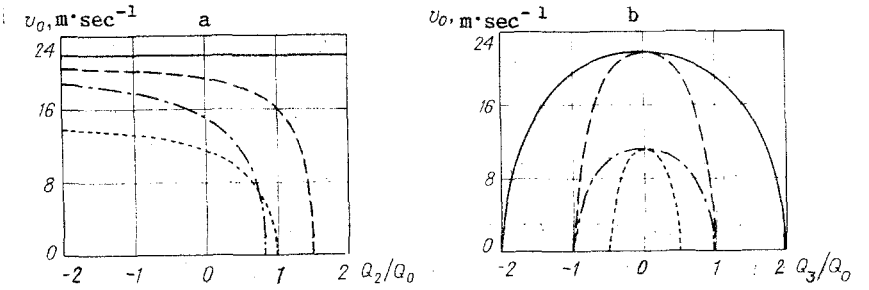

Fig. 1

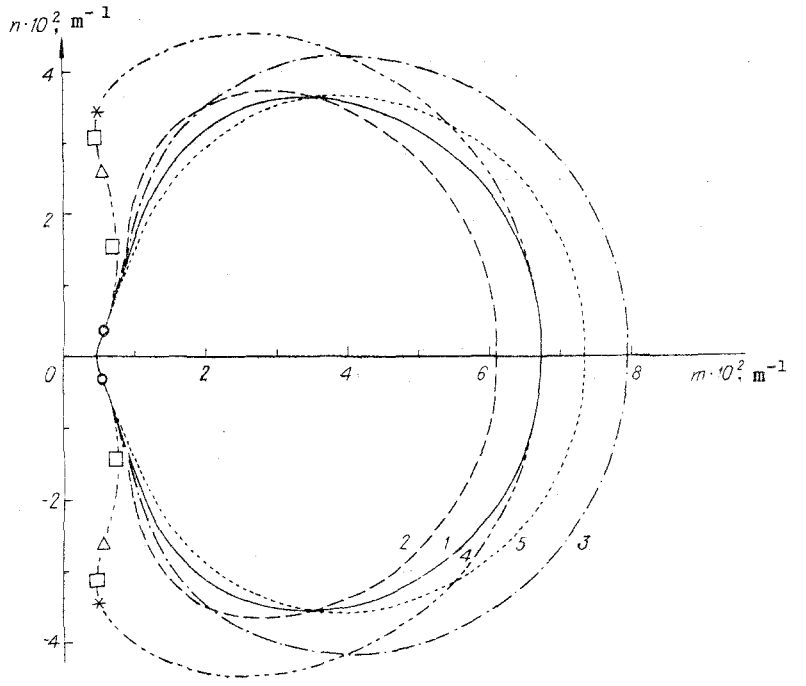

Fig. 2

in relation to r and v (a prime indicates derivative with respect to r). With uniform compression an equation for v_1 has been obtained in [3]. Shear forces give rise to ambiguity for the solution of set (3.1) as a result of which there are different values of v_1 for the upper v_1^* and lower v_1^0 arcs of the hodograph. If $Q_3 > 0$, then $v_1^* < v_1^0$ and $v_1^* > v_1^0$ for $Q_3 < 0$. With fulfillment of the condition $v < v_1$ there are no points of inflection in arcs of the hodograph. The area bounded by the hodograph decreases with a reduction in v contracting to the point with velocity v tending towards v_0.

With an increase in v the area of the hodograph between the circles contracts to a point approaching the origin with v tending towards c. For $v > c$ the hodograph passes through the origin and only one point of inflection marked with a triangle is retained on the arcs. Here tangents to the arcs at the origin form with the abscissa axis an angle $\psi = \pm\arctan\sqrt{(v/c)^2 - 1}$. The distance between the points of intersection of the hodograph with axis m increases (decreases) with an increase in longitudinal compression (tension). Transverse compression deforms the hodograph so that in it (with fulfillment of the condition $m' = m'' = 0$) points may appear with a tangent perpendicular to the abscissa axis. They are marked with squares. In the absence of shear compression these points appear if

$$Q_1 \geqslant Q_1^*, \quad Q_1^* = Q_2 - \tau_1(r^*, Q_2),$$

$$\tau_1(r, Q_2) = v^2\left(\varkappa_1 + \frac{1}{rg\,\mathrm{th}\,rH}\right)\left[1 - \frac{1 - Q_2 r^2 + D_1 r^4}{2r^2\left(2D_1 r^2 - Q_2\right)}\left(1 - \frac{2rH}{\mathrm{sh}\,2rH}\right)\right],$$

where r^* is the positive root of the equation

$$\tau_2(r, Q_2) + 2\tau_3(r, Q_2) = 0, \quad \tau_2 = (2rH + \mathrm{sh}\,2rH)\left(4Q_2 r - 6D_1 r^3 - \tau_1\tau_4'\right).$$

$$\tau_3 = (Q_2 - 4D_1 r^2)\, r\,\mathrm{sh}\,2rH - (1 + D_1 r^4 - Q_2 r^2 - \tau_1\tau_4)(3 - 2\,rH\,\mathrm{th}\,rH)\,H,$$

$$\tau_4 = (1 + D_1 r^4 - Q_2 r^2)\left[v^2 + (\varkappa_1 v^2 - \tau_1)\, rg\,\mathrm{th}\,rH\right]^{-1} rg\,\mathrm{th}\,rH.$$

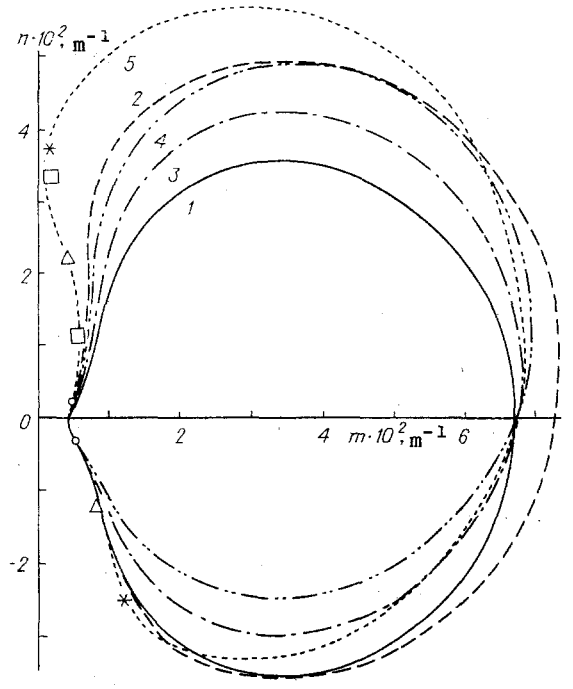

Fig. 3

Distributions of Q_1^* with respect to Q_2 are illustrated in Fig. 4 where curves 1 and 2 relate to values of source velocity of 30 and 45 m·sec^{-1}, and solid and broken lines are given for basin depths of 350 and 50 m. Curves $Q_1^*(Q_2)$ for different v intersect at a point corresponding to $Q_1^* = Q_2$. This value coincides with the critical force Q^* under conditions of uniform compression [3, 4, 7]. If the waves are short, then $Q^* = \sqrt{20}/3\ Q_0$. In the case of long waves $Q^* = \sqrt{3}Q_0$. A reduction in basin depth leads to a marked increase in Q^*.

Under conditions of shear compression there is no symmetry for the position of points with a vertical tangent with respect to the abscissa axis for the upper and lower arcs of the hodograph. Here it is only possible for these points to be present in one of the arcs (curve 5 in Fig. 3).

4. Differentiation of the equation for the line of equal phase $mx + ny = \text{const}$ with respect to r and R shows orthogonality of the group velocity vector towards the tangent of the hodograph and phase velocity towards the crest (trough) of a wave. In order to build up a phase portrait of wave disturbances along the direction of the group velocity we plot a section of length $2\pi k[r\cos(\theta - \gamma)]^{-1}$ ($\theta = \arctan(m/n)$, $\gamma = \arctan[dG/dn(dG/dm)^{-1}]$, k is equal phase line number).

We analyze the structure of the phase portraits for the corresponding hodographs. With $v_0 < v < c$ the section of the arc of the hodograph (see Figs. 2 and 3) to the right of the asterisk characterizes a bent wave ahead of the source, and to the left a bent-gravity wave following behind it [3]. If here $v > v_1$, then the outer normals to the points marked by circles specify the outer boundaries, and the triangles specify the inner boundaries of the angular zones of a ship's wake with three-wave disturbances [3]. Between these inner boundaries disturbances are only formed by transverse gravity waves. Bent waves in a wave trail are characterized by sections of arcs between triangles and asterisks, and those running ahead of the source by sections to the right of the asterisks. With absence of shear forces the structure of the phase portraits is qualitatively the same as with uniform compression [3, 4]. In addition , growth of Q_1 reduces the length of waves (bent to a greater extent than gravity waves) in the track of source movement.

The zone of the wave trail only covered by transverse waves contracts with an increase in compressive force Q_2 as a result of a shift in the inner boundaries of the region with three-wave disturbances; with $Q_1 = Q_1^*$ it disappears. With a further increase in compressive forces the boundaries in question retreat beyond the track. As a result of this in the vicinity of the track there is superimposition on each of the other parts of the right-hand and left-hand zones with three wave systems [3]. Disturbances in the overlap zone are shown

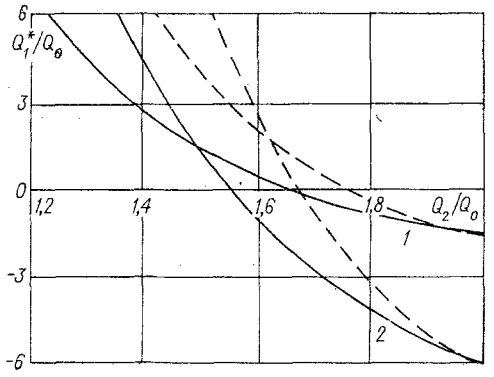

Fig. 4

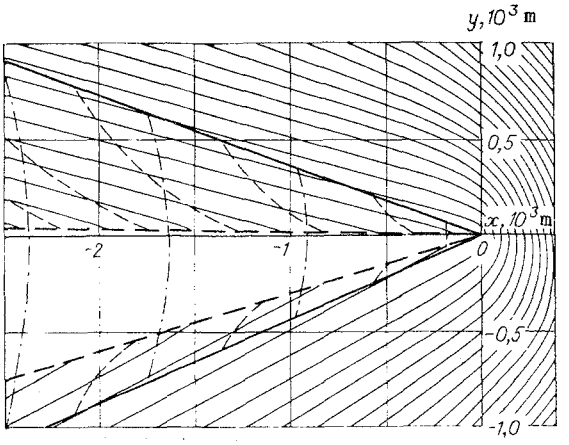

Fig. 5

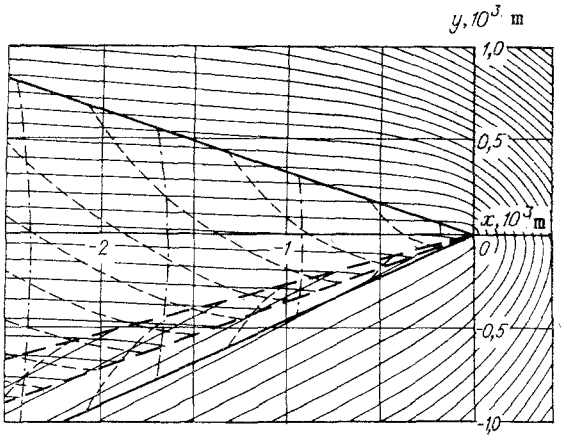

Fig. 6

in Figs. 2 and 3 by areas of the hodograph between the triangles. Rectangles close to the abscissa axis correspond to intersection of the crest by a longitudinal wave, and those at a distance correspond to intersection of bent waves with the track. Displacement of the outer boundary of the region of three-wave disturbances under the influence of Q_2 is insignificant. Force Q_1 also has a weak effect on the size of angular zones.

Phase pictres of wave disturbances under conditions of shear compression ($Q_3 > 0$) corresponding to hodographs 2 and 5 from Fig. 3 are presented in Figs. 5 and 6 with $\max(v_1^*, v_1^0) < v < c$. The outer and inner boundaries of the angular zones are shown by bold solid

and broken lines. Bent, longitudinal, and transverse waves relate to thin solid, broken, and broken-dotted lines. Asymmetry of the wave trail in relation to the movement course of the source can be seen. The angular zone with three-wave disturbance (Fig. 5) to the left with respect to the course is greater than to the right. Its inner boundary is arranged closer to the track converging with it with an increases in both Q_3 and Q_2. Values of compressive forces Q_3 and Q_2 are possible such that this boundary moves beyond the track whereas the inner boundary of the right-hand zone does not reach the track (Fig. 6).

Phase pictures with $Q_3 < 0$ are symmetrical with those provided for $Q_3 > 0$ in relation to the track. It is noted that with $Q_3 > 0$ in the range $v_1^0 < v < v^*$ and angular zone for generation of the three systems of waves only arises to the left, and for $v_1^* < v < v_1^0$ when $Q_3 < 0$ to the right of the track along the direction of source movement. With $v > c$ transverse gravitation waves are not created in the wake behind the source.

5. Now let the source move through drifting ice at an angle α to the direction of the drift. We turn the coordinate system at angle $\beta = \arctan [(u \sin \alpha)/(v + u \cos \alpha)]$. In the system obtained the source will move with velocity $U_0 = [(v + u \cos \alpha)^2 + (u \sin \alpha)^2]^{1/2}$ along the new abscissa axis and longitudinal, transverse, and shear forces take the values

$$Q_{1\beta} = Q_1 \cos^2 \beta + Q_2 \sin^2 \beta + Q_3 \sin 2\beta,$$
$$Q_{2\beta} = Q_1 \sin^2 \beta + Q_2 \cos^2 \beta - Q_3 \sin 2\beta,$$
$$Q_{3\beta} = (1/2)(Q_2 - Q_1) \sin 2\beta + Q_3 \cos 2\beta.$$

Analysis of the hodograph of the wave vector and the phase structure of wave disturbances in the new coordinate system is carried out as with absence of flow for $v = U_0$, $Q_i = Q_{i\beta}$, $i = 1, 2, 3$.

LITERATURE CITED

1. A. E. Bukatov, "Effect of longitudinal compression on nonsteady-state oscillation of drifting ice," Mor. Gidrofiz. Issled., No. 1 (1980).
2. A. D. Kerr, "The critical velocities of a moving source on a floating ice plate that is subjected to in-plane forces," Gold. Reg. Sci. Tech., No. 6 (1983).
3. A. E. Bukatov and A. A. Yaroshenko, "Effect of a uniformly compressed floating elastic plate on the development of three-dimensional waves in a uniform liquid," Izv. Akad. Nauk SSSR, Mekh. Zhidk. Gaza, No 6 (1984).
4. R. M. S. M. Schulkes, R. J. Hosking, and A. D. Sneyd, "Waves due to a steadily moving source on a floating ice plate," J. Fluid. Mech., 180, 297 (1987).
5. J. W. Davis, R. J. Hosking, and A. D. Sneyd, "Waves due to a steadily moving source on a floating ice plate," J. Fluid. Mech., 158, 269 (1985).
6. T. Takizawa, "Response of a floating ice sheet to a steadily moving load," J. Geophys. Res., 93, No. C5 (1988).
7. A. E. Bukatov, "Effect of ice compression on unsteady bent-gravity waves," Okeanologiya, 20, No. 4 (1980).
8. V. V. Bogorodskii and V. P. Gavrilo, Ice. Physical Properties. Modern Methods in Glaciology [in Russian], Gidrometeoizdat, Leningrad (1980).
9. D. E. Kheisin, Ice Cover Dynamics [in Russian], Gidrometeoizdat, Leningrad (1967).